Nonlinear Photonic Crystals

V. Berger

Thomson CSF Laboratoire Central de Recherches, Domaine de Corbeville, 91400 Orsay, France

(Received 19 June 1998)

Nonlinear frequency conversion in 2D $\chi^{(2)}$ photonic crystals is theoretically studied. Such a crystal has a 2D periodic nonlinear susceptibility, and a linear susceptibility which is a function of the frequency, but constant in space. It is an in-plane generalization of 1D quasi-phase-matching structures and can be realized in periodic poled lithium niobate or in GaAs. An interesting property of these structures is that new phase-matching processes appear in the 2D plane as compared to the 1D case. It is shown that these in-plane phase-matching resonances are given by a *nonlinear Bragg law*, and a related nonlinear Ewald construction. Applications as multiple-beam second-harmonic generation (SHG), ring cavity SHG, or multiple wavelength frequency conversion are envisaged. [S0031-9007(98)07386-4]

PACS numbers: 42.70.Qs

During the last decade, a large effort has been devoted to understanding the propagation of electromagnetic waves in photonic crystals (PC) [1–4]. These materials are artificial structures with a periodic dielectric function. One intriguing issue of PCs is the possible existence of photonic band gaps (PBGs), i.e., frequency ranges where propagation of light is forbidden inside the structure [5,6]. The Bragg mirror, as a multilayer periodic stack of two different materials, is the simplest example of 1D PC, and PBG materials can be viewed as a generalization of Bragg mirrors in several dimensions.

Some work has been devoted to the nonlinear properties of PCs, in particular, $\chi^{(2)}$ processes [7–9]. All these studies have dealt with regular PCs, having a periodic linear susceptibility $\chi^{(1)}$. In contrast with these previous studies, this paper will focus on the possibilities offered by a $\chi^{(2)}$ photonic crystal. Such a structure presents a space-independent linear dielectric constant, but has a periodic second-order nonlinear coefficient. Figure 1 shows schematically an example of the structure under study: a 2D triangular lattice of cylinders with nonlinear susceptibility tensor $(-\chi^{(2)})$ in a medium of nonlinear susceptibility $\chi^{(2)}$.

In the same way as the 1D case of a $\chi^{(1)}$ crystal is the Bragg mirror, the 1D case of a $\chi^{(2)}$ crystal is the well-known quasi-phase-matching (QPM) structure. This structure was proposed in a pioneering paper on frequency conversion [10], in order to solve the problem of phase mismatch. In a second-order nonlinear frequency conversion process, the linear dispersion of the crystal mismatches the phases between the different interacting optical waves. This reduces the useful interaction length for frequency conversion to the so-called "coherence length," which is inversely proportional to the dispersion and equal to $L_c = \lambda_0^\omega/4(n^{2\omega} - n^\omega)$ for SHG of a wavelength λ_0^ω in vacuum. QPM consists of reversing the sign of the nonlinear susceptibility of the material every coherence length. The consequence is the change of sign of the nonlinear polarization, which exactly compensates for the destructive interference coming from the dispersive propagation. The constructive buildup of the generated wave occurs then on the entire length of the QPM structure, increasing the overall energy conversion [11].

Various demonstrations of QPM have been performed (for a review, see [11]). For instance, GaAs waveguides with periodic (100) and (−100) oriented zones were recently demonstrated [12], and periodically poled lithium niobate (PPLN) [13] or periodic poled KTP [14] have recently become some of the most attractive nonlinear materials for optical parametric oscillators.

The first point addressed in this paper concerns the possibility of realizing a 2D or 3D $\chi^{(2)}$ photonic crystal. In 1D QPM structures, for GaAs waveguides as for PPLN, the 1D periodicity of the nonlinear susceptibility is defined by the design of a metallic grating. In the case of GaAs waveguides, the grating is used as a mask for a reactive ion etching step [12], and in the case of PPLN, the grating is an electrode for ferroelectric domain

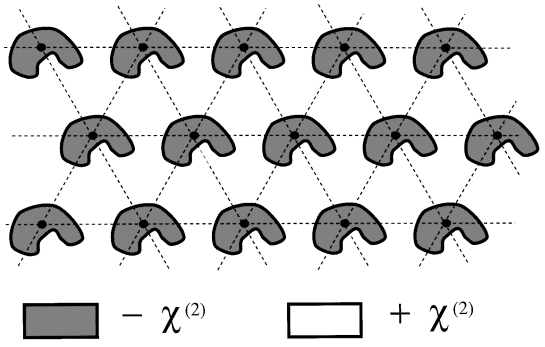

FIG. 1. Schematic picture of a 2D $\chi^{(2)}$ crystal. The material presents a translation invariance perpendicular to the figure, and is invariant by translation in a 2D lattice (here a triangular lattice). The linear susceptibility is constant in the whole material but the sign of the second-order susceptibility $\chi^{(2)}$ presents a given pattern in the unit cell. Such a material can be realized in PPLN or in GaAs, by means of state-of-the-art technology.

 0031-9007/98/81(19)/4136(4)$15.00

reversal. Though these techniques are very different, they both use a metallic grating, defined by electron-beam lithography, which defines the pattern of the QPM structure. Both techniques can be generalized to the 2D structure presented in Fig. 1. One has only to change the metallic grating into a metallic honeycomb mask during the technological process. In the case of PPLN, it is necessary to choose a connected area for the metal (white area in Fig. 1), in order to apply easily the voltage on the whole pattern. We conclude that 2D $\chi^{(2)}$ photonic crystals are easy to obtain as a generalization of 1D QPM technology.

Conversely, the fabrication of 3D $\chi^{(2)}$ crystals seems to be very tricky. One may imagine a complicated multistep technology with bondings, etchings, and regrowth of GaAs, resulting in a 3D stack of domain reversals. Such a process, theoretically possible, is, however, far beyond the state-of-the-art of GaAs technology. For this reason, this paper will consider mainly 2D $\chi^{(2)}$ crystals. However, it is clear that a hypothetical 3D structure would present analogous properties to those described here, and the assumption of a 2D structure in the following is not a loss of generality.

Let us assume that a plane wave at the frequency ω propagates in the transverse plane of a 2D $\chi^{(2)}$ crystal that is perpendicular to the translation axis of the cylinders, of arbitrary section. Let us recall that the linear dielectric constant is constant in the whole structure. This ensures that multiple reflections, leading to PBG effects, are not present. In this 2D structure, the problem can be considered as scalar [15], which simplifies the notations. For instance, in the case of a 2D PPLN crystal, fundamental and harmonic waves are TM polarized, i.e., with the electric field in the translational direction. Although they are constant in space, the linear dielectric constants are assumed to be different at ω and 2ω, this dispersion being the source of phase mismatch. An efficient SHG process in the $\chi^{(2)}$ crystal is obtained if a quasi-plane-wave at the harmonic frequency is observed to increase at a large scale, compared to the coherence length L_c and to the $\chi^{(2)}$ period order. By quasi-plane-wave, it is assumed that if we write the harmonic electric field as

$$\mathcal{E}^{2\omega}(\mathbf{r},t) = \tfrac{1}{2} E^{2\omega}(\mathbf{r}) \exp[i(2\omega t - \mathbf{k}^{2\omega}\mathbf{r})] + \text{c.c.}, \quad (1)$$

then the classical slow varying envelope approximation applies:

$$\mathbf{k}^{2\omega} \cdot \nabla [E^{2\omega}(\mathbf{r})] \gg \nabla^2 E^{2\omega}(\mathbf{r}). \quad (2)$$

In these equations, $\mathbf{r} \equiv (x, y)$ is the 2D spatial coordinate. Under this assumption, the evolution of the SH field amplitude can be written as a function of the pump field and the second-order coefficient $\chi^{(2)}(\mathbf{r})$:

$$\mathbf{k}^{2\omega} \cdot \nabla [E^{2\omega}(\mathbf{r})] = -2i \frac{\omega^2}{c^2} (E^{\omega})^2 \chi^{(2)}(\mathbf{r}) \exp[i(\mathbf{k}^{2\omega} - 2\mathbf{k}^{\omega})\mathbf{r}]. \quad (3)$$

This equation is a simple generalization in two dimensions of the 1D harmonic field evolution equation [16], where the derivative has been replaced by a gradient and $(E^{\omega})^2$ is assumed to be constant. The nonlinear susceptibility can be written as a Fourier series,

$$\chi^{(2)}(\mathbf{r}) = \sum_{\mathbf{G} \in \mathrm{RL}} \kappa_{\mathbf{G}} \cdot \exp(-i\mathbf{G} \cdot \mathbf{r}), \quad (4)$$

where the sum is extended over the whole 2D reciprocal lattice (RL) [17]. Inserting this expression in Eq. (3), the increase of the SH field appears to be related to a sum of $\exp[i(\mathbf{k}^{2\omega} - 2\mathbf{k}^{\omega} - \mathbf{G})\mathbf{r}]$. The QPM condition appears then as the expression of the momentum conservation,

$$\mathbf{k}^{2\omega} - 2\mathbf{k}^{\omega} - \mathbf{G} = \mathbf{0}. \quad (5)$$

For 1D QPM, the phase mismatch can be compensated in a structure of period d if it is equal to a multiple of the fundamental spatial frequency of the structure $\frac{2\pi}{d}$ [11]. In contrast to this, QPM in a 2D $\chi^{(2)}$ photonic crystal involves a momentum taken in at the 2D RL. The possibilities of QPM are not only sixfold degenerate (thanks to the symmetry of the triangular lattice), but new QPM orders appear in the 2D crystal which are not multiples of the fundamental QPM process, opposite to the 1D situation. Two examples of 2D QPM processes are shown in Fig. 2: the fundamental process, which involves the shortest possible $\mathbf{G}$ vector, and a 2D QPM process with a momentum transfer $\sqrt{3}$ times greater, which is impossible in a 1D structure. The 2D QPM order can be

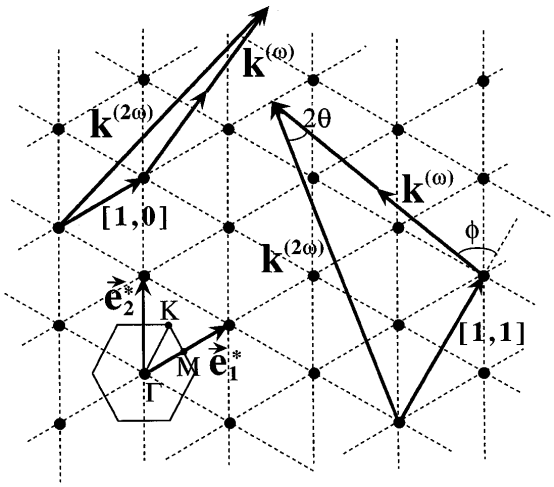

FIG. 2. Reciprocal lattice of the structure of Fig. 1, with the 2D QPM processes of order $[1,0]$ and $[1,1]$ shown schematically. The efficiency of the nonlinear process is proportional to the corresponding 2D Fourier series coefficient, which depends on the unit cell filling factor, and is not represented here. The first Brillouin zone with the usual Γ, M, and K points is represented on the left.

labeled with two integer coordinates, given in the $(\mathbf{G}_1, \mathbf{G}_2)$ basis of the RL. In Fig. 2, for instance, 2D QPM processes of orders $[1,0]$ and $[1,1]$ are represented. In the case of a unit cell invariant by the symmetry operations of the Bravais lattice (as, for instance, a triangular lattice of circular patterns), it is obvious that points in a 30° sector ΓM-ΓK form a complete set of QPM schemes, all other points in the RL playing the same role for a reason of symmetry. This means that $[x, y] \in N^2$ orders with $y \geq 0$ and $x - \sqrt{3}\, y \geq 0$ represent all the 2D QPM processes in these structures. In the case of an asymmetric unit cell (as, for example, the graphitelike structure [19]), the RL and the QPM schemes are the same as above. However, the related conversion efficiency depends on the Fourier coefficient of Eq. (4), which depends on the shape of the $\chi^{(2)}$ pattern at the unit cell level, and is generally not the same for different vectors of equal modulus in the RL.

A particularly interesting case occurs when $\mathbf{k}^{2\omega}$ and $\mathbf{k}^{\omega}$ are collinear, because the interaction length is not limited by the walk-off between pump and harmonic waves. Such a process is obtained when the phase mismatch is equal to the modulus of a vector in the RL. For instance, in the case of a structure with a triangular lattice of period d, the phase mismatches that can be compensated are equal to $\sqrt{x^2 + y^2 + xy} \times \frac{2\pi}{d}$, $[x, y] \in N^2$. They are then belonging to the series $(1, \sqrt{3}, 2, \sqrt{7}, 3, 2\sqrt{3}, \ldots)$. This has to be compared to the series $(1, 3, 5, 7, \ldots)$ which is obtained in the usual 1D QPM process.

Using some trigonometry, Fig. 2 leads to

$$\lambda^{2\omega} = \frac{2\pi}{|\mathbf{G}|} \sqrt{\left(1 - \frac{n^{\omega}}{n^{2\omega}}\right)^2 + 4\,\frac{n^{\omega}}{n^{2\omega}}\,\sin^2\theta}\,, \qquad (6)$$

where $\lambda^{2\omega}$ is the SH wavelength inside the material and 2θ the walk-off angle between $\mathbf{k}^{2\omega}$ and $\mathbf{k}^{\omega}$ [20]. More generally, this equation gives the direction of coherent radiation at the wavelength $\lambda^{2\omega}$ for a phased array of nonlinear dipoles having a phase relation fixed by the propagation of the pump. Equation (6) appears then as a *nonlinear Bragg law,* and is a generalization for nonlinear optics of the Bragg law. It gives the direction of resonant scattering at the wavelength $\lambda^{2\omega}$ of a plane wave with vector $\mathbf{k}^{\omega}$ by a set of nonlinear dipoles. If the medium has no dispersion, $n^{\omega} = n^{2\omega}$ and Eq. (6) is reduced to the well known Bragg law, which expresses the resonant scattering direction by a periodic set of scatterers,

$$\lambda = \frac{4\pi}{|\mathbf{G}|}\,\sin(\theta) = 2d\,\sin(\theta)\,, \qquad (7)$$

where d is the period between two planes of scatterers. In the case $n^{\omega} = n^{2\omega}$, the nonlinear emission follows the same behavior as a linear scattering: In both cases the direction of propagation is given by the Huyghens-Fresnel principle, given the phase relation between the scatterers.

The analogy with x-ray diffraction by crystals is useful for understanding the different possibilities offered by 2D QPM. Figure 3 shows a modified Ewald construction corresponding to Eq. (6). This figure follows the same principle as the usual Ewald construction, except for the fact that the radius of the Ewald sphere $|\mathbf{k}^{2\omega}|$ is greater than the distance $2|\mathbf{k}^{\omega}|$ between its center and the origin of the RL. As in the case of x-ray diffraction, for a given pump wave vector $\mathbf{k}^{\omega}$, there is in general no reciprocal vector $|\mathbf{k}^{2\omega}|$ on the Ewald sphere. This means that the 2D QPM is a resonant process, an "accident," which can be obtained by varying either the angle of propagation of the pump or the wavelength. It is interesting to note that for specific angles and wavelengths several points can be located simultaneously on the Ewald sphere. In such a case of multiple resonance, SH beams can be generated simultaneously in different directions in the plane, in a similar way as the linear diffraction in several order beams by a diffraction grating. These different beams will present anticorrelation noise properties which can be useful in quantum optics experiments.

The new possibilities offered by $\chi^{(2)}$ photonic crystals can be classified into two categories: First, for a given pump frequency ω, a phase-matched direction in the lattice is required for an efficient SHG. In that case, by changing the angle of incidence in the structure, the Ewald sphere crosses for some angle a point of the RL. For this direction, phase matching occurs resonantly in a very similar way as a Bragg resonance in a rotating crystal x-ray diffraction experiment. The walk-off of the nonlinear interaction corresponding to this resonance is given by the nonlinear Bragg law (6). For a unit cell having the same symmetry as the crystal, as explained before, several directions of propagation are equivalent. This can be used for ring cavity purposes. At variance with previous ring cavity nonlinear optics experiments [21], a ring cavity (having the shape of a hexagon, for instance) can be designed so

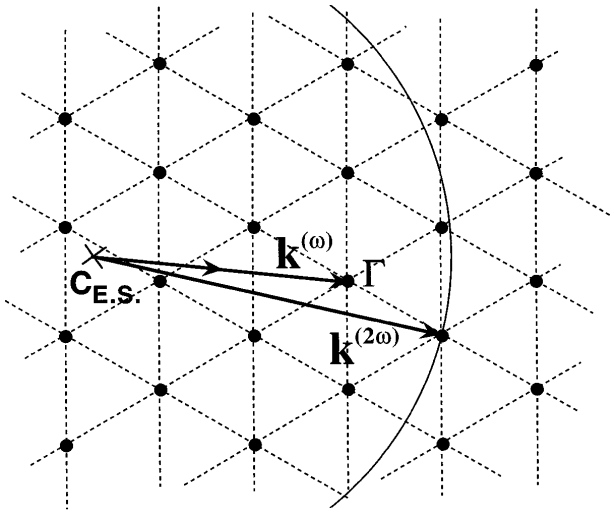

FIG. 3. Nonlinear Ewald construction: The center of the Ewald sphere is located $2\mathbf{k}^{\omega}$ away from the origin of the RL and the radius of the sphere is $\mathbf{k}^{2\omega}$. The main difference with the usual Ewald construction is that the Ewald sphere does not contain the origin of the RL. If a point of the RL is located on the Ewald sphere, phase matching occurs for the SHG process.

that the constructive interaction occurs along in the entire intracavity optical path, increasing the final efficiency. The lower efficiency coming from the structure factor [17] is overcome by the increase of the interaction length on the entire cavity round trip in the 2D case.

A second application is the search of the phase-matched SHG spectrum, for a given direction of propagation. The x-ray analog of this kind of experiment is the broadband x-ray diffraction analysis used in the Laue method [22]. The different QPM resonances are found from the scheme of Fig. 3 by changing the radius of the Ewald sphere. It is obvious that several resonances will be found; this opens the possibility of multiple wavelength generation by SHG. It is interesting to compare this phenomenon with multiple wavelength SHG that has been recently obtained in a quasiperiodic 1D Fibonacci optical superlattice [23]. Multiple resonances were observed in the QPM SHG spectrum arising from the different reciprocal vectors $G_{m,n}$ of the quasiperiodic optical superlattice. The 2D RL indexing of the quasiperiodic 1D structure is the fundamental difference from the usual 1D periodic structure, and this difference is the reason for multiwavelength frequency conversion. The 2D indexing comes from the fact that the 1D quasiperiodic lattice is nothing but the projection of a 2D periodic crystal on a 1D axis. This follows the well known geometrical construction of quasicrystalline structures. The experiments of Zhu and coworkers [23] are thus a projection of a 2D $\chi^{(2)}$ PC experiment on one particular direction of propagation. 1D QPM experiments are also such a projection but the difference is the following: in the 1D QPM case, the propagation is on such an axis that the $\chi^{(2)}$ function is periodic on this axis, whereas in the quasiperiodic structure the projection is done on an axis with an irrational slope. All these cases are contained in the 2D $\chi^{(2)}$ photonic crystal, and can be obtained by changing the angle of propagation in the 2D plane of the material.

The author is deeply indebted to Giuseppe Leo, Carlo Sirtori, and Børge Vinter for a critical reading of the manuscript.

[1] *Confined Electrons and Photons: New Physics and Applications*, edited by C. Weisbuch and E. Burstein (Plenum, New York, 1995).

[2] *Photonic Band Gap Materials*, edited by C. Soukoulis (Plenum, New York, 1995).

[3] J. D. Joannopoulos, R. D. Meade, and J. N. Winn, *Photonic Crystals* (Princeton University Press, Princeton, 1995).

[4] V. Berger, Opt. Mater. **11**, 131–142 (1998).

[5] E. Yablonovitch, Phys. Rev. Lett. **58**, 2059 (1987).

[6] E. Yablonovitch, T. J. Gmitter, and K. M. Leung, Phys. Rev. Lett. **67**, 2295 (1991).

[7] K. Sakoda and K. Ohtaka, Phys. Rev. B **54**, 5742 (1996).

[8] J. Martorell, R. Vilaseca, and R. Corbalan, Appl. Phys. Lett. **70**, 702 (1997).

[9] A. Fiore, V. Berger, E. Rosencher, P. Bravetti, and J. Nagle, Nature (London) **391**, 463 (1997).

[10] J. A. Armstrong, N. Bloembergen, J. Ducuing, and P. S. Pershan, Phys. Rev. **127**, 1918 (1962).

[11] M. M. Fejer, G. A. Magel, D. H. Jundt, and R. L. Byer, IEEE J. Quantum Electron. **28**, 2631 (1992).

[12] S. J. B. Yoo *et al.*, Appl. Phys. Lett. **68**, 2609 (1996).

[13] L. E. Myers *et al.*, Opt. Lett. **20**, 52 (1995); J. Opt. Soc. Am. B **12**, 2102 (1995).

[14] H. Karlsson and F. Laurell, Appl. Phys. Lett. **71**, 3474 (1997).

[15] P. R. Villeneuve and M. Piché, Phys. Rev. B **46**, 4969 (1992).

[16] A. Yariv, *Quantum Electronics* (John Wiley & Sons, New York, 1989).

[17] In the case of the honeycomb lattice of cylinders, following [18], $\kappa_{\mathbf{G}} = 4f\frac{J_1(|\mathbf{G}|R)}{|\mathbf{G}|R} \times \chi^{(2)}$, where f is the filling factor of the circle in the Wigner-Seitz cell, and J_1 is the first Bessel function. For a radius R of cylinders equal to 0.38 times the period, we have $\kappa_{\mathbf{G}} = 0.13\chi^{(2)}$ for a $[1,0]$ order process. This can be compared to $\frac{2}{\pi}\chi^{(2)}$ in the case of a 1D first order QPM. Higher $[1,0]$ Fourier coefficients can be obtained with a triangular lattice of hexagons instead of cylinders.

[18] V. Berger, O. Gauthier-Lafaye, and E. Costard, J. Appl. Phys. **82**, 60 (1997).

[19] D. Cassagne, C. Jouanin, and D. Bertho, Phys. Rev. B **53**, 7134 (1996).

[20] Using simple trigonometric transformations, Eq. (6) can also be written as a function of the angle ϕ between $\mathbf{k}^{\omega}$ and $\mathbf{G}$:

$$\lambda^{2\omega} = \frac{2\pi}{|\mathbf{G}|}\left(\sqrt{1 - \left(\frac{n^{\omega}}{n^{2\omega}}\right)^2 \sin^2\phi} - \frac{n^{\omega}}{n^{2\omega}}\cos\phi\right).$$

This form has not been given in this paper because the analogy with the Bragg law is not apparent at all here. However, this expression has another interest: it leads to the relation between ϕ, $\lambda^{2\omega}$, and d for 1D QPM, away from normal incidence. By just setting $md = \frac{2\pi}{|G|}$, where m is the order of the 1D QPM, Eq. (32) of Ref. [11] is found again.

[21] W. J. Kozlovsky, C. D. Nabors, and R. L. Byer, IEEE J. Quantum Electron. **24**, 913 (1988).

[22] C. Kittel, *Introduction to Solid State Physics* (John Wiley & Sons, New York, 1976).

[23] S. N. Zhu *et al.*, Phys. Rev. Lett. **78**, 2752 (1997).